CHAPTER VI
CATALYTIC ACTIVITY AND STABILITY OF HZSM-5 AND HIERARCHICAL UNIFORM MESOPOROUS MSU-S$_{ZSM-5}$ DURING BIO-ETHANOL DEHYDRATION

6.1 Abstract

Many zeolites have been used in the transformation of bio-ethanol into hydrocarbons such as HZSM-5, HBeta, and HY, especially for HZSM-5 that has moderate pore size and moderate acidity. Recently, many researchers had studied on mesoporous catalysts in the dehydration of bio-ethanol due to their high diffusivity. In this work, HZSM-5 and its hierarchical mesoporous MSU-S$_{ZSM-5}$ were studied for their catalytic stability in bio-ethanol dehydration. The reaction was conducted in a U-tube fixed bed reactor at 450 °C for 4 days. The results showed that propane selectivity decreased, and ethylene, propylene, and mixed C4 increased in the gas from HZSM-5 catalyst whereas the gas product of MSU-S$_{ZSM-5}$ was mostly composed of ethylene. Moreover, HZSM-5 still maintained the production of large hydrocarbons such as C$_9$ and C$_{10+}$ aromatics along with 96 hours of TOS because its pore size was less proper for coke deposition. On the other hand, for MSU-S$_{ZSM-5}$, the selectivity of C$_{10+}$ aromatic fraction decreased along with TOS due to coke deposition. Furthermore, the spent catalysts were examined for their textural properties. HZSM-5 showed the better catalytic activity and textural properties than that of MSU-S$_{ZSM-5}$, indicating by a lower % decrease in surface area, lower amount of coke deposited, lower decrease in acidity, and no dealumination during 4 days of bio-ethanol dehydration.

6.2 Introduction

Nowadays, the replacement of non-renewable energy is one of the high priority issues. Many researchers had been studying on production of alternatives energy from renewable materials. Bio-ethanol is one of the renewable sources that its usage can reduce greenhouse gas released to environment. Bio-ethanol can be

used as gasoline or diesel blender to be gasohol or bio-diesel. Moreover it can be converted to hydrocarbons via catalytic dehydration of bio-ethanol. Many catalysts had been studied for the catalytic dehydration of bio-ethanol, and one of the most active catalysts in this reaction is HZSM-5. In 2005, Takahara *et al.* used HZSM-5, HBeta, HY, HMOR, and silica alumina in ethanol dehydration. They found that most of gaseous products were ethylene, ethane, diethyl ether, propylene, and butylenes. A year later, Inaba *et al.*, (2006) found that HZSM-5 had the highest potential to produce benzene, toluene, and xylenes among the four zeolites previously employed. For producing heavier liquid products, conventional microporous catalysts such as zeolites limit the diffusion of large molecules. Recently, mesoporous catalysts such as MCM-41 have been investigated to overcome the weakness of microporous catalysts (Karlsson *et al.*, 1999). However, because of its poor framework stability and poor acidity, the mesoporous catalyst was not capable to be used as a catalyst.

Mesoporous zeolites can be divided into three categories; that are, (a) hierarchical zeolites, (b) nano-crystal sized zeolites, and (c) supported zeolites (Egeblad *et al.*, 2008). The hierarchical zeolites are the ones that have additional meso-porosity in each crystal, and also have intercrystalline pore, normally defined as macropore. The nano-crystal sized zeolites typically have crystal sizes below 100 nm. Either intracrystalline or intercrystalline systems can be found in the nano-crystal sized zeolites, defined as the micropore and mesopore system, respectively. The last category is supported zeolites, defined as those of which are supported or dispersed in the pore of another material. In addition, Ramasamy *et al.* (2014) synthesized nano-crystal size HZSM-5 with mesopores created from stacked nano-crystals (Type (b) above), and compared its stability with that of a conventional HZSM-5 at the same Si/Al ratio during ethanol dehydration to hydrocarbons. From TPO experiments, at a low Si/Al ratio (40), the life time of the nano-crystal sized HZSM-5 was 2 times longer than that of the conventional HZSM-5. Moreover, the nano-crystal sized HZSM-5 was 1.6 times higher coke formation than the conventional zeolite. At a high Si/Al ratio (140), the nano-crystal sized HZSM-5 had 5 times longer life time than the conventional HZSM-5 and 2.1 times higher amount of coke deposited. It was found that the nano-crystal size HZSM-5 gave higher actual/theoretical oil yield and higher olefinic compound than the conventional

HZSM-5. Moreover, it exhibited the higher catalytic stability than the conventional one at all Si/Al ratios.

In 2001, Liu *et al.* synthesized the hierarchical mesoporous MSU-S with ZSM-5 (MSU-S$_{ZSM-5}$) and Beta (MSU-S$_{BEA}$) seeds (Mesoporous zeolites of Type a). The results showed that MSU-S$_{MFI}$ and MSU-S$_{BEA}$ provided the higher hydrothermal stability and cumene cracking activity than Al-MCM-41. Moreover, MSU-S had been used in other reactions. Triantafyllidis *et al.*, (2007) studied MSU-S$_{BEA}$ for biomass pyrolysis, and stated that the MSU-S$_{BEA}$ selectively produced polycyclic aromatic hydrocarbons, and provided higher aromatic yields than Al-MCM-41 due to its stronger acid sites. For the catalytic dehydration of bio-ethanol, the hierarchical mesoporous MSU-S$_{BEA}$ also has been studied by Sujeerakulkai and Jitkarnka (2014). The synthesized MSU-S$_{BEA}$ with Si/Al$_2$ ratio of 81 possessed the large pore size of about 2.72 nm and the high surface area of around 580 m^2/g. The results from bio-ethanol dehydration exhibited that ethylene was the major component in the gas stream whereas C$_{10+}$ aromatics was the main component in the oil composition, followed by C$_9$ aromatic and xylenes. Moreover, methanol dehydration by using the hierarchical mesoporous MSU-S$_{ZSM-5}$ was studied by Rashidi *et al.* (2013) aiming to produce dimethyl ether (DME). The synthesized MSU-S$_{ZSM-5}$ with SiO$_2$/Al$_2$O$_3$ ratio of 55 gave 100 % DME selectivity in that temperature range of 200 – 320 °C, which was higher than that obtained from Al-MCM-41. Therefore, it is evident that both HZSM-5 and the hierarchical mesoporous catalyst with ZSM-5 seed can be potentially used as a catalyst for catalytic dehydration of bio-ethanol. The hierarchical mesoporous MSU-S$_{ZSM-5}$ with a uniform hexagonal structure might improve the higher amount of large hydrocarbons with uniform products than a non-uniform mesoporous catalyst that has no uniformity of the structure leading to the non-uniform products. In this work, microporous HZSM-5 and a hierarchical mesoporous MSU-S$_{ZSM-5}$ were studied in bio-ethanol dehydration in order to investigate the product distribution and catalytic activity with time-on-stream (TOS). The reaction was conducted at 450 °C under atmospheric pressure for 4 days.

6.3 Experimental

6.3.1 Catalyst Preparation

6.3.1.1 Synthesis of MSU-S_{ZSM-5}:

The synthesis of MSU-S_{ZSM-5} was achieved using the method developed by Liu et al., 2001: Rashidi et al., 2013. 10.2 g of tetrapropyl ammonium hydroxide (TPAOH, 40 %wt) was mixed with 79.26 g of deionized water. Then, 6.0 g of fumed silica and 0.34 g of sodium aluminate as a silicon and aluminum source were sequentially added into the solution of TPAOH and deionized water. The solution was then stirred at 50 °C for 18 hours to form the ZSM-5-seed containing solution. After that, 9.44 g of CTAB were mixed with 100 g of deionized water, and mixed with the solution of ZSM-5-seed. The final gel was kept in a Teflon-lined autoclave for the hydrothermal treatment at 150 °C for 2 days to form the mesoporestructure. Then, the final gel was filtered, washed, and dried. The obtained white powder was ion exchanged with 0.1M NH_4NO_3 in 96 % ethanol at 80 °C reflux temperature for 2 hours. The final catalyst was dried, and calcined at 1 °C/min to 550 °C kept for 10 hours. Then, the calcined MSU-S_{ZSM-5} was pelletized, crushed, and sieved into 20 - 40 mesh particles before use in the reactor.

6.3.1.2 Commercial Zeolites

HZSM-5 zeolite (MFI, NH_4-form, SiO_2/Al_2O_3 = 30 mol/mol, BET surface area = 340 m^2/g, Zeolyst International, USA) was used in this work. HZSM-5 was calcined at 500 °C, 10 °C/min for 4 hours to obtained the H-form and remove the impurities. Then, the calcined catalyst was hydraulically pressed to pellets. Next, the pellets were crushed and sieved to 20 - 40 mesh particles before use in the reactor. The abbreviations of catalysts used in the experiment are shown in Table 6.1.

6.3.2 Catalyst Characterization

The surface area (BET), pore volume (Horvath Kawazoe method), and pore size (Barret-Joyner-Halenda method) were determined based on N_2 physisorption using the Thermo Finnigan/Sorptomatic 1990. The X-ray Diffraction (XRD) patterns of the zeolites were determined using Rigaku SmartLab® in

BB/Dtex mode with CuKα radiation. For the small-angle mode, the machine collected the data from 1° – 7° at 1°/min. For the wide-angle mode, the machine collected the data from 5° – 50° at 5°/min with the increment of 0.01. The bulk and surface Si/Al_2 ratios of the synthesized MSU-S_{ZSM-5} were determined by X-ray Fluorescence spectrometry (XRF) and X-ray Photoelectron Spectroscopy (XPS), respectively. X-ray fluorescence spectrometry (AXIOS PW4400) was used to determine the bulk Si/Al ratio of the fresh and spent catalysts. The conditions were set as follows: internal flow of 4.10 l/min, external flow of 2.49 l/min, cabinet temperature of 29.97 °C, primary temperature of 19.00 °C, vacuum of 10.10 Pa, x-ray generation of 50 kV (60 mA), 150 μm of collimator, angle of 10.0002 degree, gas flow 0.90 l/h, and gas pressure of 1020.8 hPa. XPS was used to determine the Si/Al ratio on the surface of the fresh and spent catalysts. The scan pass energy was 160 kV for wide scan and 40 kV for narrow scan. The electron source was Al Kα that gave 10 mA of emission and 15 kV of anode HT. The neutralizer was set at 1.8 A of filament current, 2.6 V of charge balance, and 1.3 V of filament bias. Temperature Programmed Desorption (TPD-NH_3) was also used to determine the acidity of the catalysts. Acid properties such as acid strength and acidity were determined by Thermo Finnigan 1100. 0.2 g of a catalyst was treated by nitrogen flow at 300 °C for 3 hours. Then, after the catalyst was cooled down to room temperature, it was added with 10 % v/v NH_3 of helium balance with a flow of 20 ml/min. The NH_3-TPD profiles were obtained by heating the reactor at 10 °C/min up to 800 °C with a helium flow of 20 ml/min. After that, the desorbed gases were analyzed by a TCD detector. Transmission Electron Microscopy (TEM) was used to determine the hexagonal structure of MSU-S_{ZSM-5}. The mixture of a catalyst powder and ethanol was sonicated for 20 min. After that, the mixture was dropped onto copper grid with a Formvar support, and then dried. Hitachi H-7501 SS in TEM high-resolution (HR) mode took images using a voltage of 100 kV. In addition, the coke formation on catalysts was determined by a Thermogravimetric/Differential Thermal Analyzer (TG/DTA). The spent catalysts were weighed and placed in a Pt pan followed by heating from 50 to 900 °C with the heating rate of 10 °C /min. Nitrogen and oxygen flow rates were controlled at 100 ml/min and 200 ml/min, respectively.

Table 6.1 Nomenclature of catalysts used in the experiments

# of run	Catalyst	Abbreviation
1	HZSM-5 at 1 day time-on-stream	HZ-S1
2	HZSM-5 at 2 days time-on-stream	HZ-S2
3	HZSM-5 at 3 days time-on-stream	HZ-S3
4	HZSM-5 at 4 days time-on-stream	HZ-S4
5	MSU-S$_{ZSM-5}$ at 1 day time-on-stream	MSU-Z-S1
6	MSU-S$_{ZSM-5}$ at 2 days time-on-stream	MSU-Z-S2
7	MSU-S$_{ZSM-5}$ at 3 days time-on-stream	MSU-Z-S3
8	MSU-S$_{ZSM-5}$ at 4 days time-on-stream	MSU-Z-S4

6.3.3 Bio-ethanol Dehydration

99.5 % purity of bio-ethanol was obtained from Sapthip Co. Ltd.,. The catalytic dehydration of bio-ethanol was performed in a U-tube fixed bed reactor under atmospheric pressure at 450 °C for 24, 48, 72, and 96 hours by collecting data at every 4 hours and using 3 g of catalyst. Bio-ethanol was fed at 2 ml/hour and mixed with helium co-fed at 13.725 ml/min. The ethanol concentration was determined by a GC-FID (Agilent 6890N), and gas compositions were analyzed by a GC-TCD (Agilent 6890N). The liquid product was condensed in the collector in an ice bath. Then, CS_2 was used to extract the oil from the liquid products. After that, SIMDIST GC was used to determine the true boiling point curve of oil. The range of boiling point indicates the type of petroleum products:<149 °C for gasoline, 149-232 °C for kerosene, 232-343 °C for gas oil, 343-371 °C for light vacuum gas oil, and >371 °C for high vacuum gas oil (Dũng et al., 2009). The oil composition was determined by using Gas Chromatograph equipped with a Mass Spectrometry of "Time of Flight" type (GC×GC- TOF/MS) (installed with Rxi-5SilMS and RXi-17 consecutive columns). The conditions were set as follows: the initial temperature of 50 °C held for 30 minutes, the heating rate of 2 °C/min from 50 to 120 °C, and 10 °C/min from 120 to 310 °C with split ratio of 5.

6.4 Results and Discussion

6.4.1 Catalyst Characterization of HZSM-5 and MSU-S$_{ZSM-5}$

The Small Angle X-Ray Scattering (SAXS) patterns of the hierarchical mesoporous MSU-S$_{ZSM-5}$ was determined by using Rigaku TTRAX in the small angle (1-7°) mode and the XRD patterns in wide-angle (5-50°) mode by using Rigaku Smartlab® are shown in Figures 6.1. MSU-$_{ZSM-5}$ provides a sharp peak around 2.2° and a broad peak around 22° which indicate that MSU-S$_{ZSM-5}$ with a hexagonal structure was successfully synthesized with a semi-crystalline structure. The result from XRF shows that HZSM-5 and MSU-S$_{ZSM-5}$ have the Si/Al$_2$ ratio of 28 and 39.6, respectively. The lower Si/Al$_2$ ratio of HZSM-5 indicates that HZSM-5 seeds have been embedded in the highly Si-containing structure of MSU-S$_{ZSM-5}$.

Next, Figure 6.2(a) exhibits the N$_2$ adsorption-desorption isotherm of MSU-S$_{ZSM5}$, which illustrates the same suddenly-increasing step at P/P$_0$ nearby 0.35 as found in the Al-MCM-41 case (Triantafyllidis *et al.*, 2007) indicating that MSU-S$_{ZSM-5}$ has two pore sizes in the structure. Furthermore, the pore size distribution in Figure 6.2(b) shows that the hierarchical mesoporous MSU-S$_{ZSM5}$ has both micropore and mesopore, which is different from HZSM-5 that has only micropore. The micropore and mesopore diameters of MSU-S$_{ZSM5}$ determined by using H.K. and B.J.H methods are 7.10 and 29.6 Å, respectively. Moreover, Table 6.2 exhibits the surface area, pore size, and pore volume of HZSM-5 and MSU-S$_{ZSM-5}$ using Horvath Kawazoe and Barret-Joyner-Halenda method. It can be noted that the synthesized MSU-S$_{ZSM-5}$ provides three times higher surface area and pore volume than the conventional HZSM-5.
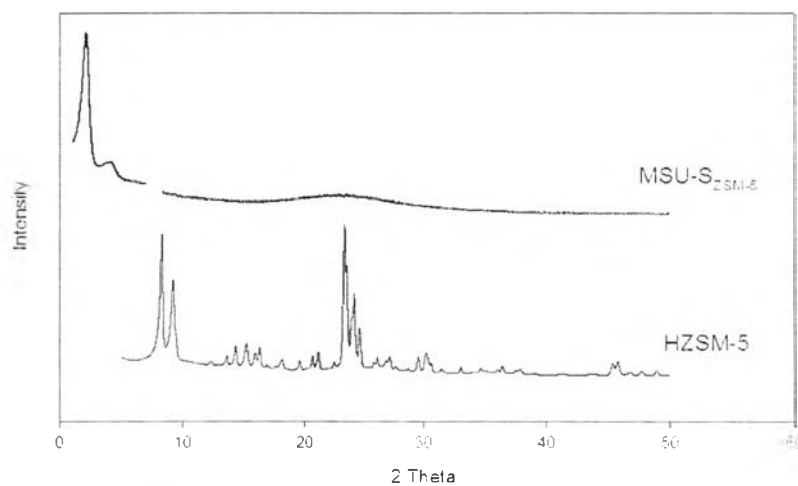
Figure 6.1 XRD patterns of MSU-S$_{ZSM-5}$ and HZSM-5.
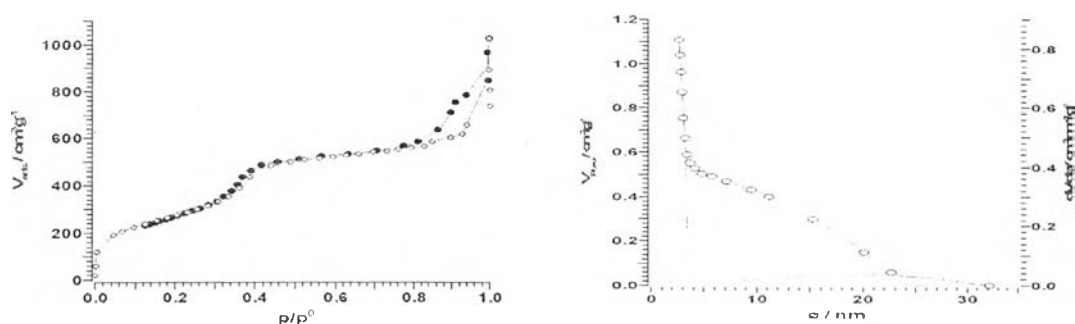
Figure 6.2 (a) N$_2$ adsorption-desorption isotherm, and (b) Pore size distribution of MSU-S$_{ZSM5}$ using B.J.H method.
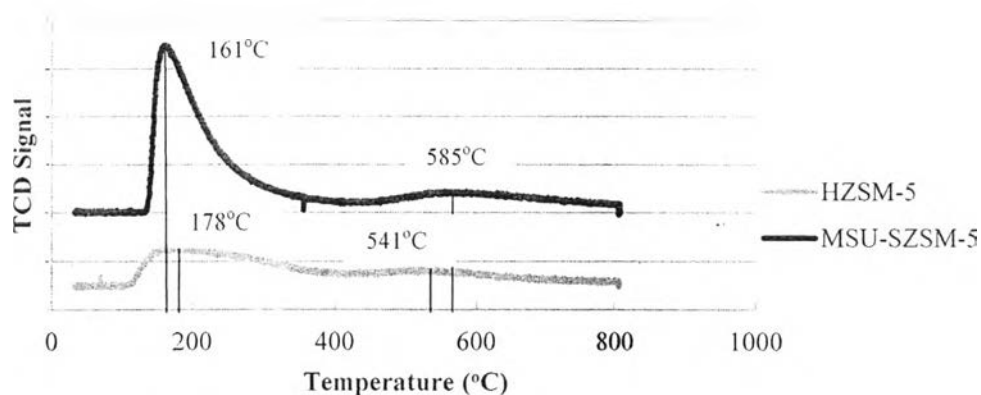
Table 6.2 Physical properties of HZSM-5 and MSU-S$_{ZSM-5}$

Catalysts	Si/Al$_2$ Ratio	Surface Area (m^2/g)^a	Pore Volume (cm^3/g)^b	Micropore Diameter (Å)^b	Mesopore Diameter (Å)^c
HZSM-5	28.0	361.2	0.31	7.54	-
MSU-S$_{ZSM-5}$	39.6	1,028	1.02	7.10	29.6

^{a} Determined by BET method. ^{b} Determined by H.K. method. and ^{c} Determined by B.J.H method

Furthermore, the acidity of HZSM-5 and MSU-S$_{ZSM-5}$ were determined by using TPD-NH$_3$. The results in Figure 6.3 show that both catalysts exhibit two peaks, which mean they have two types of acid sites: that are, weak and strong acid sites. MSU-S$_{ZSM-5}$ exhibits a peak at 161 ^{o}C, possibly a weak Lewis acid site or silanol group and another peak at 585 ^{o}C, possibly a strong Bronsted acid site, whereas HZSM-5 provides a similar weak acid site at 178 ^{o}C and a strong Bronsted acid site at 541 ^{o}C. Moreover, HZSM-5 has the stronger Lewis acid site than MSU-S$_{ZSM-5}$ as indicated by the higher temperature of the Lewis acid peak. However, MSU-S$_{ZSM-5}$ has stronger Bronsted acid site than HZSM-5. Furthermore, MSU-S$_{ZSM-5}$ has both higher Lewis and Bronsted acid densities than those of HZSM-5 as indicated by the larger area under the peaks. Acid density is strongly affected by Si/Al$_2$ ratio of the catalyst. The higher amount of Si atom of MSU-S$_{ZSM-5}$ gave the higher density of Lewis acid site (or silanol group) whereas the Bronsted acid density of both catalysts are not significantly different


**Figure 6.3** TPD-NH$_3$ profiles of HZSM-5 and MSU-S$_{ZSM-5}$.

6.4.2 Stability of HZSM-5 and MSU-S$_{ZSM-5}$

The spent HZSM-5 and MSU-S$_{ZSM-5}$ catalysts were characterized to determine their textural properties. Figure 6.4(a) and (b) illustrate the XRD and SAXS patterns of HZSM-5 and MSU-S$_{ZSM-5}$. It can be noted that the XRD patterns of spent HZSM-5 catalysts at various TOSs are about the same as the fresh one. Moreover, the relative crystallinity is almost constant at 100 %, meaning that the

structure and crystallinity of HZSM-5 are maintained along time-on-stream. The SAXS patterns of spent MSU-S$_{ZSM-5}$ show a lower intensity and a little shift to larger angles with increasing TOS, indicating that it has smaller pore size and poorer pore structure alignment (Thanabodeekij *et al.,* 2006). So. it can be concluded that the structures of both HZSM-5 and MSU-S$_{ZSM-5}$ are not destroyed during 4 days of bio-ethanol dehydration. Moreover. X-ray Photoelectron Spectroscopy (XPS) and X-ray Fluorescence (XRF) were used to determine the surface and bulk Si/Al$_2$ ratio of HZSM-5 and MSU-S$_{ZSM-5}$. respectively. The surface Si/Al$_2$ ratios were obtained from the normalized area of the Si 2p and Al 2p signals. The plot of variation of surface Si/Al$_2$ vs bulk Si/Al$_2$ ratios is employed to determine the dealumination of the catalyst (Moreno and Poncelet, 1997). The variation of surface Si/Al$_2$ vs bulk Si/Al$_2$ ratios of HZSM-5 at various TOSs illustrated in Figure 6.5(a) indicates that the data points are located nearby the diagonal line, meaing that Si/Al$_2$ at the surface and bulk of the spent catalysts are about the same as the fresh ones, and therefore HZSM-5 is not dealuminated during 4 days of bio-ethanol dehydration. Furthermore, Figure 6.5(b) shows the variation of surface Si/Al$_2$ vs bulk Si/Al$_2$ ratios of MSU-S$_{ZSM-5}$ located above the diagonal line, indicating that the Si/Al$_2$ at the surface is higher than the one in the bulk. It is evident that aluminum atom is not present at the outer surface of MSU-S$_{ZSM-5}$, but it is in the inner surface of the hexagonal structure. Additionally, MSU-S$_{ZSM-5}$ is not also dealuminated during 4 days of bio-ethanol dehydration.
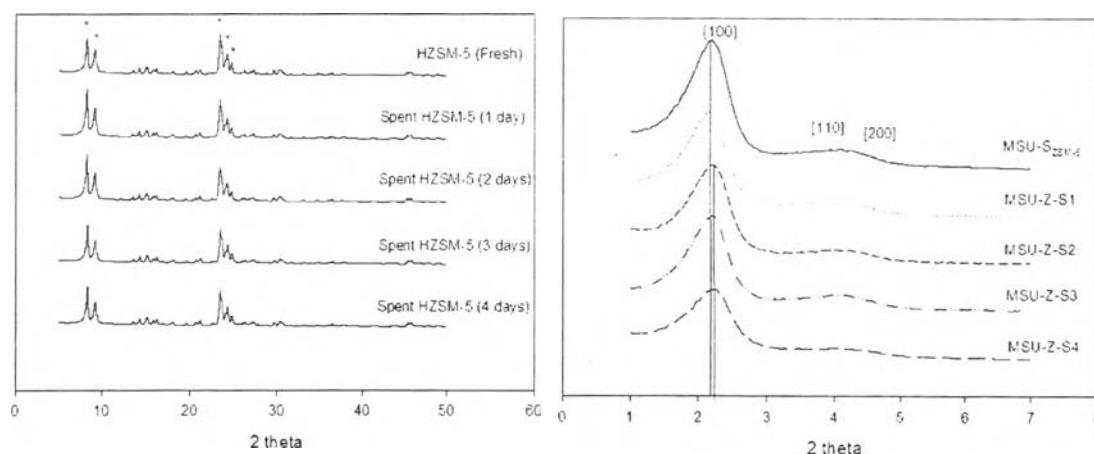

**Figure 6.4** (a) XRD patterns of HZSM-5 and (b) SAXS patterns of MSU-S$_{ZSM-5}$.
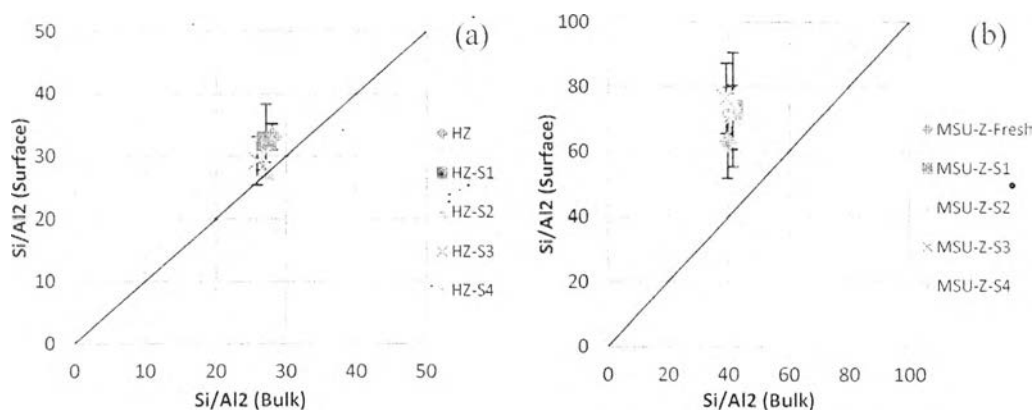
Figure 6.5 Variation of surface Si/Al_2 vs. bulk Si/Al_2 ratios of (a) HZSM-5, and (b) MSU-S$_{ZSM-5}$.

Moreover, the decreases of surface area and pore volume of spent HZSM-5 and MSU-S$_{ZSM-5}$ are shown in Figure 6.6(a) and (b). It can be stated that the moderate pore size and moderate acidity of HZSM-5 do not much allow the formation of coke molecules, which can be seen from the gradual decreases of surface area and pore volume along TOS. Meanwhile, the large pore size and high acid density of MSU-S$_{ZSM-5}$ are favored for the formation of polyaromatics that can be condensed and deposit on the acid sites, which cause a coke deposition. So, they affect to the higher % decrease in the surface area and pore volume of MSU-S$_{ZSM-5}$. Additionally, Figure 6.7 exhibits the coking rate of HZSM-5 and MSU-S$_{ZSM-5}$, and indicates that both catalysts have a high coking rate at the beginning, but it decreases with increasing TOS, which means both catalysts have decreasing surface activity as the accumulated coke increases with increasing TOS. Furthermore, the TPD-NH$_3$ profiles of fresh and spent HZSM-5 and MSU-S$_{ZSM-5}$ are shown in Figure 6.8(a) and (b). It is clearly seen that both catalysts have the same type of acid site because their peaks are present at the same range of temperatures in the neighborhood of 200 °C and 550 °C. So, it can be noted that the acid properties of MSU-S$_{ZSM-5}$ are originated from those of ZSM-5 embedded in the structure of MSU-S. The acidity of HZSM-5 gradually decreases with increasing TOS, and decreases about 50 % whereas the acidity of MSU-S$_{ZSM-5}$ rapidly decreases after 1 day TOS, and it loses almost 85 %
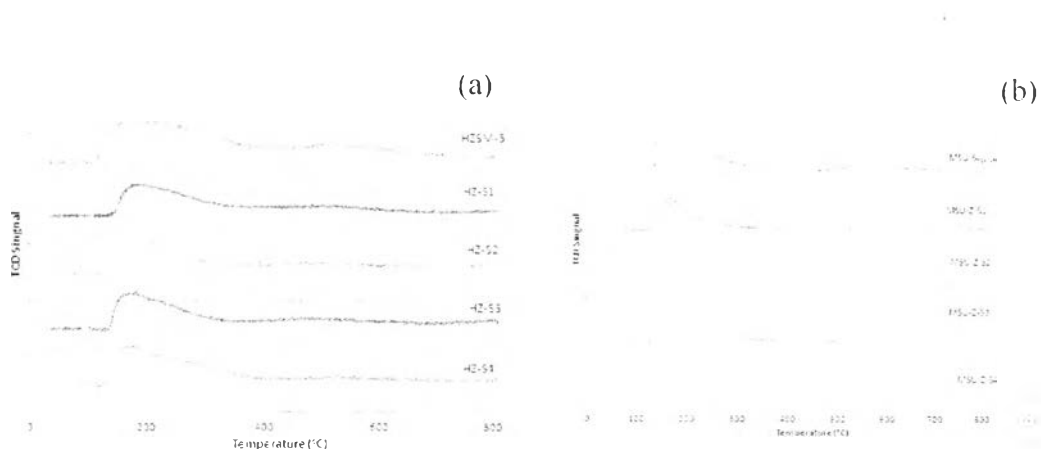
after 4 days of bio-ethanol dehydration. So. it is reasonable to conclude that HZSM-5 has better catalytic activity and textural stability than MSU-S$_{ZSM-5}$.
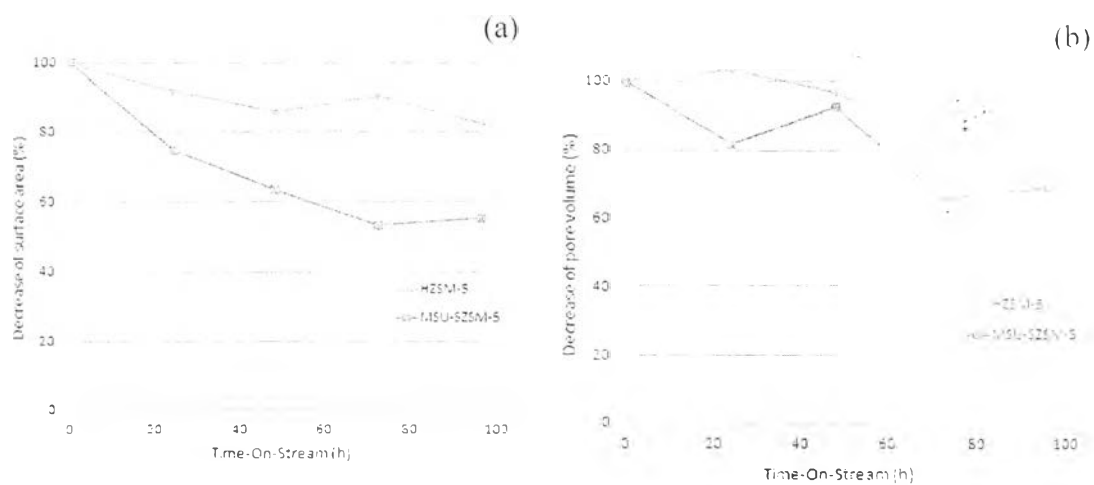
Figure 6.6 Decreases in (a) surface area (%) and (b) pore volume (%) of HZSM-5 and MSU-S$_{ZSM-5}$ with time-on-stream
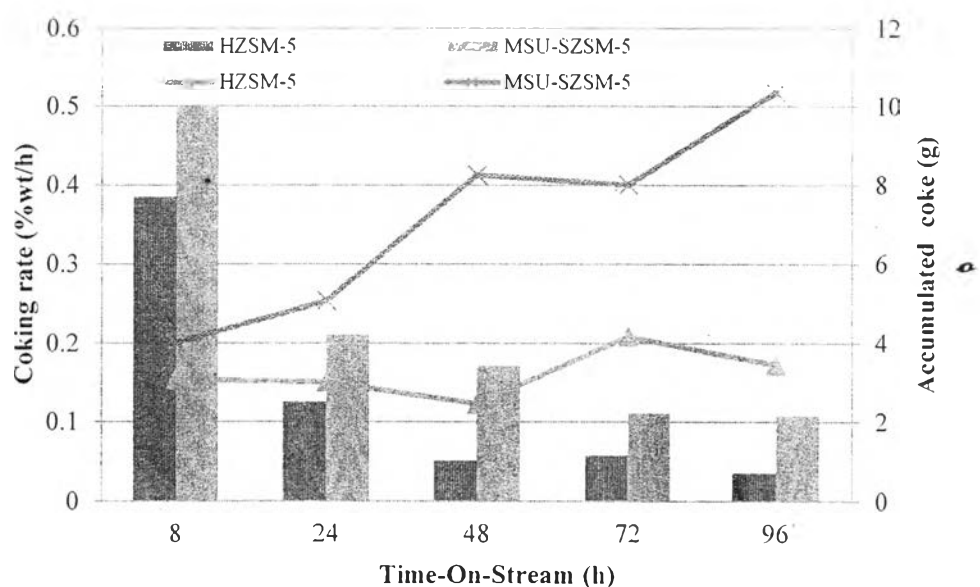
**Figure 6.7** Coking rates and accumulated coke of HZSM-5 and MSU-S$_{ZSM-5}$.

(a)   (b)

Figure 6.8 TPD-NH$_3$ profiles of (a) HZSM-5 and (b) MSU-S$_{ZSM-5}$ at various TOSs.

6.4.3 Comparison of HZSM-5 and MSU-S$_{ZSM-5}$ as Catalysts

6.4.3.1 Conversion and Gas Product

Figure 6.9(a) illustrates the concentration profiles of gaseous products from using HZSM-5. The selectivity of propane decreases whereas that of ethylene, propylene, and mixed C$_4$ selectivity increases with increasing TOS. Moreover, bio-ethanol conversion slightly decreases from almost 100 % to 98.5 % along with TOS as shown in Figure 6.9(b). It can be explained that, the Brønsted acid sites are needed for hydrogen transfer reaction. but they are the first to be deactivated by coke deposition, so resulting in the increase in selectivity of ethylene. propylene, and mixed C$_4$ (Madeira et al.. 2009). Meanwhile, Figure 6.9(c) illustrates the concentration profiles of gas components from MSU-S$_{ZSM-5}$. Ethylene is the main component in the gas stream, which is stable after 20 hour TOS. Bio-ethanol conversion of MSU-S$_{ZSM-5}$ is also shown in Figure 6.9(d), which still maintains almost 100 % along TOS. .
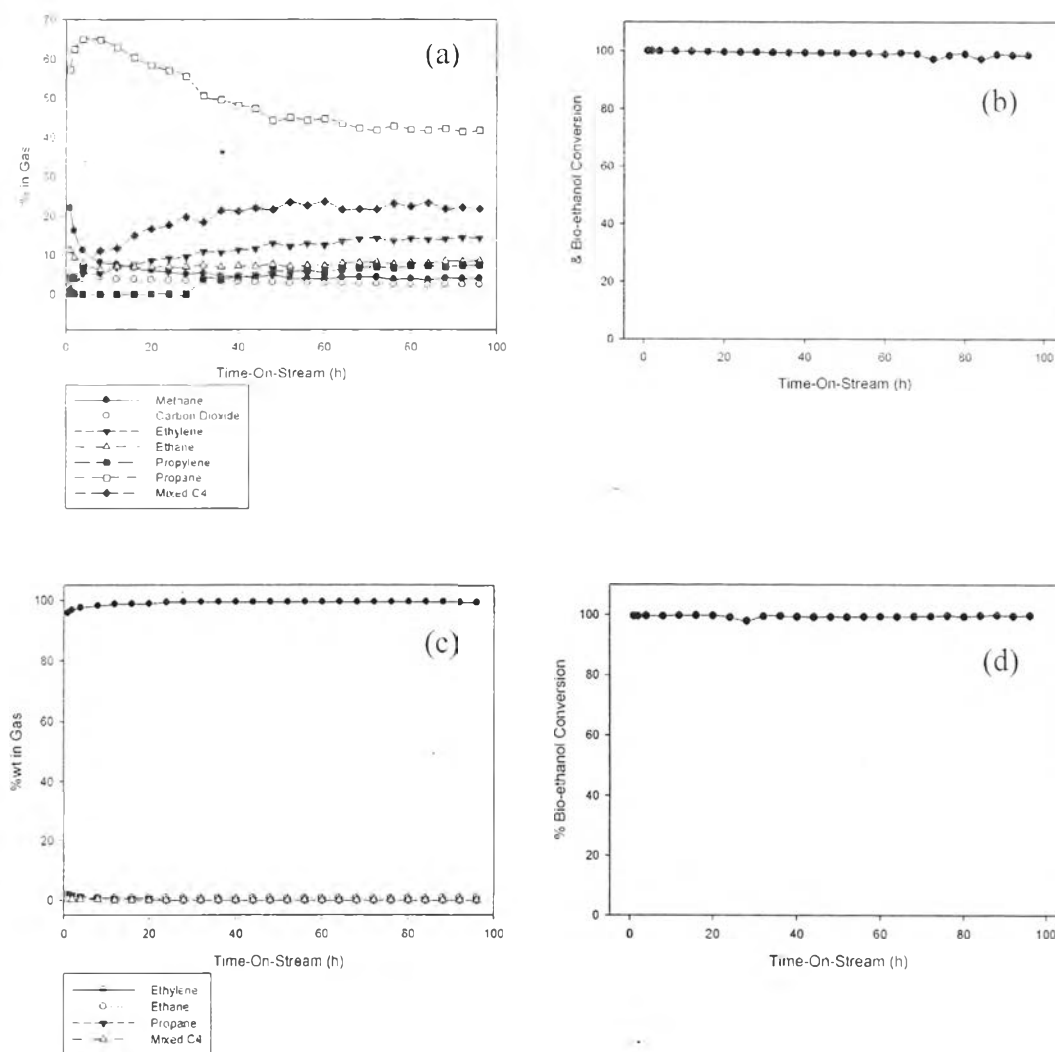
Figure 6.9 (a) Concentration profiles of gas components, (b) bio-ethanol conversion using HZSM-5 as a catalyst, (c) concentration profiles of gas components and, (d) bio-ethanol conversion from MSU-S$_{ZSM-5}$.

6.4.3.2 Petroleum Fractions of Oil

Furthermore, the petroleum fractions of the obtained oil from HZSM-5 and MSU-S$_{ZSM-5}$ at various TOSs are shown in Figure 6.10. In Figure 6.10(a), gasoline is the majority in the obtained oil from HZSM-5, followed by kerosene and gas oil due to the moderate pore size of HZSM-5 that is suitable production of hydrocarbons in the range of gasoline. As shown in Figure 6.10(b), kerosene is the majority in the obtained oil from MSU-S$_{ZSM-5}$, followed by gas oil

and gasoline due to its large pore size. As time-on-stream increases, gasoline fraction from HZSM-5 decreases whereas kerosene fraction increases, and then they keep constant after 3 days because the hydrocarbons produced from the pore of HZSM-5 can be further formed into larger molecules at the external surface area. Additionally, the selectivity of gas oil exhibits no changes after 4 days. On the other hand, the decline of gas oil fraction in the obtained oil from MSU-S$_{ZSM-5}$ arises from polyaromatics formation in the pore of MSU-S$_{ZSM-5}$, which causes coke deposition that prevents the formation of larger hydrocarbons.
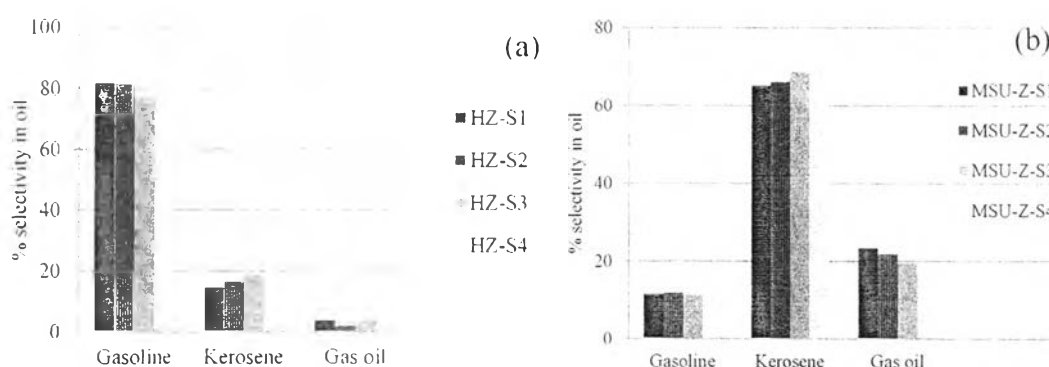

Figure 6.10 (a) Petroleum fractions from HZSM-5, and (b) MSU-S$_{ZSM-5}$ at various TOSs.

6.4.3.3 Oil Composition

Moreover, in Figure 6.11(a), the oil from HZSM-5 after 1 day TOS mostly is composed of mixed xylenes, toluene, C$_9$, and C$_{10+}$ aromatics due to its moderate pore size that is proper for the production of monoaromatics. As TOS increases, toluene can undergo dispropotionation and transalkylation, forming larger molecules such as ethylbenzene, C$_9$, and C$_{10+}$ aromatics whereas the selectivity of mixed xylenes are fluctuated among themselves, indicating isomerization reaction (Ali *et al.*, 2013) that occurs along with TOSs. The selectivities of C$_9$ and C$_{10+}$ aromatics tend to increase even after 4 days because the deactivation of HZSM-5 can only occur by coking, not by pore blocking (Pinard *et al.*, 2013) so further reactions can be also occurred at the pore mouth of the channel (Madeira *et al.*, 2009).

Meanwhile, the oil compositions of MSU-S$_{ZSM-5}$ at various TOSs are illustrated in Figure 6.11(b). MSU-S$_{ZSM-5}$ gives a high selectivity of C10$^-$ aromatics, followed by C9 aromatics and benzene at the beginning due to its large pore size. However, as TOS increases, C$_{10+}$ aromatics selectivity decreases, adversely with C$_9$ and benzene selectivity because some of C$_{10-}$ aromatics molecules can form polyaromatics that can be condensed in the pore of MSU-S$_{ZSM-5}$, which causes coking. Moreover, the acid sites have an important role on further reaction of small olefins, or aromatics, but they are covered by coke that consequently affects to the decline of C$_{10+}$ aromatics fraction.
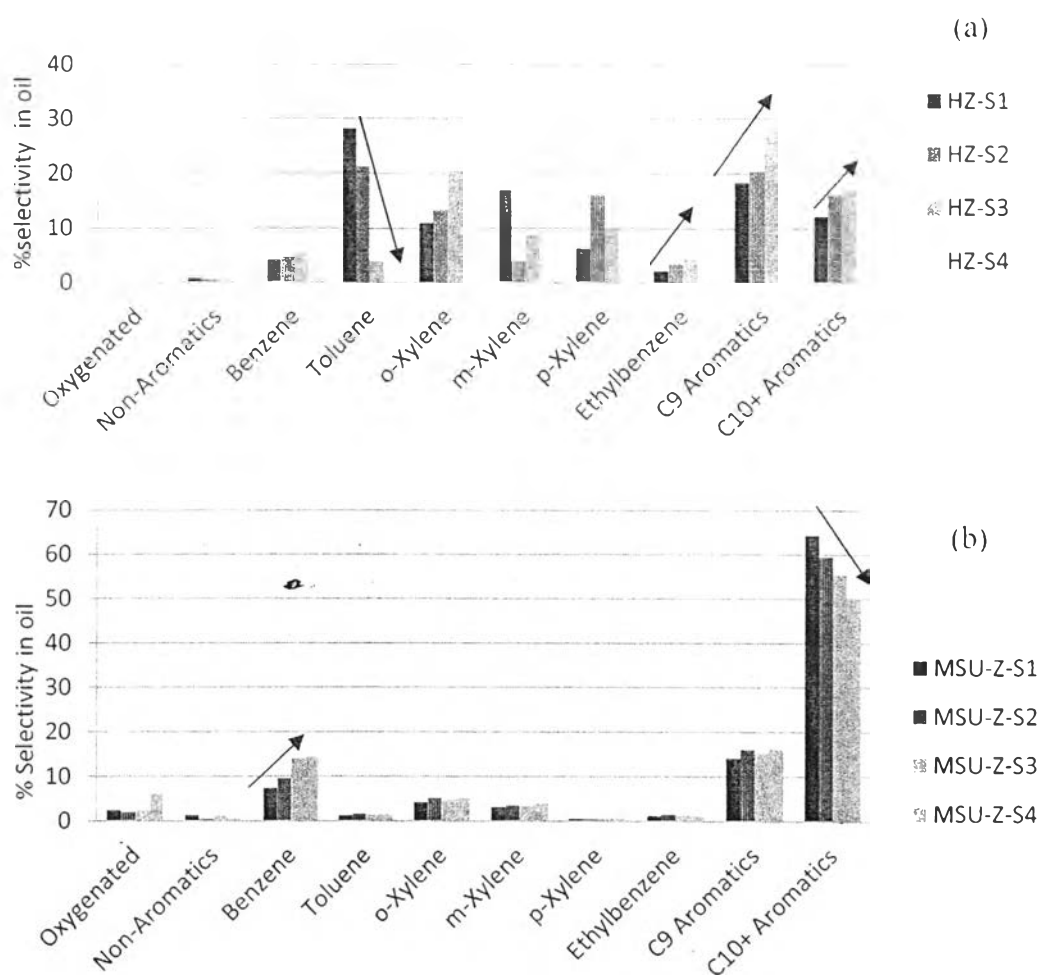
Figure 6.11 Oil compositions of HZSM-5 (a) and MSU-S$_{ZSM-5}$ (b) at various TOSs.

6.4.4 Reaction Pathways of HZSM-5 and MSU-S$_{ZSM-5}$

In terms of activity, it has been revealed that both gas and oil products from using HZSM-5 are different from that of MSU-S$_{ZSM-5}$. In the gas products, HZSM-5 gives various gas components such as propane, propylene, ethylene, methane, and mixed C$_4$ due to its small pore size and moderate acidity that is proper for oligomerization, dimerization, hydrogen transfer, and aromatization of ethylene or higher olefins. In the other hand, because of the larger pore size, MSU-S$_{ZSM-5}$ gives a high amount of ethylene in the gas products, followed by ethane, propane, and mixed C$_4$. For the oil composition of HZSM-5, toluene can undergo further reaction, forming the larger molecules such as ethylbenzene, C$_9$, and C$_{10+}$ aromatics along TOSs. Moreover, a moderate pore size and moderate acidity of HZSM-5 are not proper for the formation of polyaromatics, which can poison on the acid sites, and then affects to the high catalytic activity of HZSM-5 in terms of catalyst life time. In contrast to the oil composition from using MSU-S$_{ZSM-5}$ as a catalyst, it can be seen that C$_{10+}$ aromatics is the majority in the oil at every TOSs, and its selectivity decreases along TOS. The high acid density of MSU-S$_{ZSM-5}$ with large pore size can increase the bimolecular reactions via the increased availability of Brønsted acid site, resulting in the high selectivity of C10+ aromatics (Ramasamy and Wang, 2013). Then, C$_{10+}$ aromatics were condensed on the acid sites, which prevent the transformation of ethylene to higher hydrocarbons and cause the deactivation of the catalysts.

Additionally, using HZSM-5 as a catalyst, the reaction pathways of ethanol dehydration can be explained as follows. Ethanol is dehydrated to ethylene, and then ethylene can undergo oilgomerization reaction to form larger olefins. Next, the olefins are dehydrocyclized or hydrogenised, forming aromatics or paraffins. Moreover, Figure 6.12 shows the reactions in the micro-mesopore of HZSM-5 embedded MSU-S$_{ZSM-5}$. Monoaromatics such as toluene and xylenes or higher olefins are produced in the micropore of ZSM-5, and then, these hydrocarbons pass through the mesopore of MSU structure with a larger pore size. Monoaromatics and higher olefins can undergo alkylation, rearrangement, and hydrogen transfer to form polyaromatics, which can be condensed in the pore and cause coking. Although coke

deposited in the pore of MSU-S$_{ZSM-5}$ cannot block the pore, but it can poison the acid sites and prevents further reaction of other molecules. In contrast, HZSM-5 deactivates more slowly than MSU-S$_{ZSM-5}$ because the heavy fraction still increases even after 4 days TOS. The results from TGA showed that the amount of coke deposited on HZSM-5 are 3-4 %wt at all TOSs, which means that even HZSM-5 was saturated with coke, the further reactions can be also possible to occur at the pore mouth channel of the structure (Madeira *et al.*, 2009).
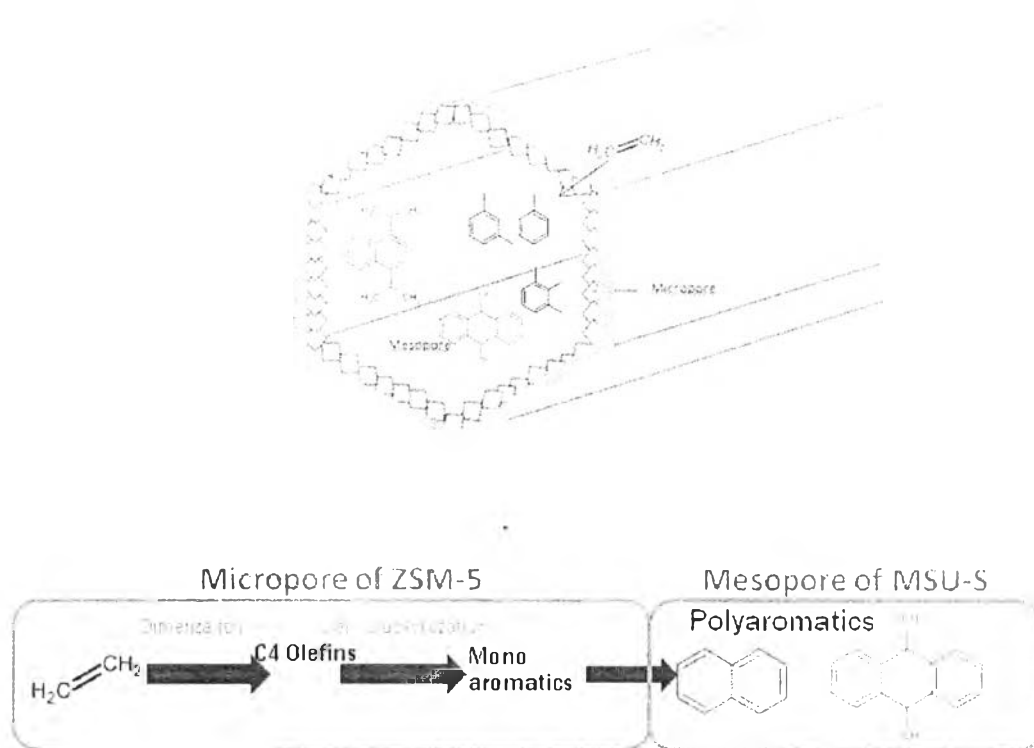
Figure 6.12 Possible reactions in micro-mesopore of MSU-S$_{ZSM-5}$.

6.5 Conclusions

Commercial HZSM-5 with Si/Al$_2$ ratio of 30 and the hierarchical mesoporous MSU-S$_{ZSM-5}$ with Si/Al$_2$ ratio of 39.6 synthesized by using TPAOH as a template and CTAB as a surfactant were used in the catalytic dehydration of bio-ethanol. The results from surface area analyzer illustrated that HZSM-5 had only one average pore size of about 7.5 Å whereas the hierarchical mesoporous MSU-S$_{ZSM-5}$

had two different pore sizes of about 7.1 Å and 29.6 Å. The gas composition from using HZSM-5 showed that propane selectivity decreased in the opposite way with ethylene, propylene, and mixed C4 due to the deactivation of Bronsted acid sites whereas the gas products from MSU-S$_{ZSM-5}$ were mostly composed of ethylene along TOS. Moreover. the selectivity of large hydrocarbons such as ethylbenzene C$_9$ and C$_{10+}$ aromatics from using HZSM-5 tended to increase with increasing TOS because further reactions such as alkylation, hydrogen transfer. and rearrangement can also be occurred at the mouth of the channels. In the other hand. the selectivity of C$_{10+}$ aromatics from using MSU-S$_{ZSM-5}$ decreased along TOS because the presence of high acid density and large pore size of MSU-S$_{ZSM-5}$ can promote the formation of polyaromatics, which can deposite on the acid sites and prevent the transformation of ethylene into higher hydrocarbons. Furthermore, the structure of both HZSM-5 and MSU-S$_{ZSM-5}$ were not destroyed during 4 days of bio-ethanol dehydration. However, HZSM-5 provided a lower % decrease in surface area, lower amount of coke deposited, and lower decrease in acidity, with no dealumination. compared to those of MSU-S$_{ZSM-5}$. So, it can be concluded that HZSM-5 had higher catalytic activity and stability than that of MSU-S$_{ZSM-5}$ during 4 days of bio-ethanol dehydration.

6.6 Acknowledgements

6.7 References

Ali, S.A., Ogunronbi, K.E., and Al-Khattaf, S.S. (2013) Kinetics of dealkylation–transalkylation of C9 alkyl-aromatics over zeolites of different structures. Chemical Engineering Research and Design, 91, 2601-2616.

Dũng, N.A., Kaewkla, R., Wongkasemjit, S., and Jitkarnka, S. (2009) Light olefins and light oil production from catalytic pyrolysis of waste tire. Journal of Analytical and Applied Pyrolysis, 86, 281-286.

Egeblad, K., Christensen, C.H., Kustova, M., and Christensen, C.H. (2008) Templating mesoporous zeolites. Chemical Materials, 20(3), 946–960.

Inaba, M., Murata, K., Saito, M., and Takahara, I. (2006) Ethanol conversion to aromatic hydrocarbons over several zeolite catalysts. Reaction Kinetics and Catalysis Letters, 88(1), 135–142.

Karlsson, A., Stocker, M., and Schmidt, R. (1999) Composites of micro- and mesoporous materials: simultaneous syntheses of MFI/MCM-41 like phases by a mixed template approach. Microporous and Mesoporous Materials, 27, 181-192.

Liu, Y., Zhang, W., and Pinnavaia, T.J. (2001) Steam-stable aluminosilicate mesostructures assembled from zeolite ZSM-5 and zeolite Beta-seeds. Angewandte Chemie International Edition, 40(7), 1255-1258.

Madeira, F.F., Gnep, N.S., Magnoux, P., Maury, S., and Cadran, N. (2009) Ethanol transformation over HFAU, HBEA and HMFI zeolites presenting similar Bronsted acidity. Applied Catalysis A, 367(1-2), 39-46.

Moreno, S. and Poncelet, G. (1997) Dealumination of small- and large-port mordenites: A comparative study. Microporous Materials, 12, 197-222.

Pinard, L., Hamieh, S., Canaff, C., Madeira, F.F., Batonneau-Gener, I., Maury, S., Delpoux, O., Ben Tayeb, K., Pouilloux, Y., and Vezin, H (2013) Growth mechanism of coke on HBEA zeolite during ethanol transformation. Journal of Catalysis, 299, 284-297.

Ramasamy, K.K., Zhang, H., Sun, J., and Wang Y. (2014) Conversion of ethanol to hydrocarbons on hierarchical HZSM-5 zeolites. Catalysis Today, 238, 103-110.

Ramasamy, K.K. and Wang, Y. (2013) Catalyst activity comparison of alcohols over zeolites. Journal of Energy Chemistry, 22, 65-71.

Rashidi, H., Hamoule, T., Nikou, M.R.K., and Shariati, A. (2013) DME synthesis over MSU-S catalyst through methanol dehydration reaction. Iranian Journal of Oil & Gas Science and Technology, 2 (4), 67-73.

Sujeerakulkai, S. and Jitkarnka, S. (2014) Bio-ethanol dehydration to hydrocarbons using Ga_2O_3/Beta zeolites with various Si/Al$_2$ ratios. Chemical Engineering Transactions, 39, 967-972.

Takahara, I., Saito, M., Inaba, M., and Murata, K. (2005) Dehydration of ethanol into ethylene over solid acid catalysts. Catalysis Letters, 105(3-4), 249-252.

Thanabodeekij, N., Sadthayanon, S., Gulari, E., and Wongkasemjit, S. (2006) Extremely high surface area of ordered mesoporous MCM-41 by atrane route. Materials Chemistry and Physics, 98, 131-137.

Triantafyllidis, K.S., Iliopoulou, E.F., Antonakou, E.V., Lappas, A.A., Wang, H., and Pinnavaia, T.J. (2007) Hydrothermally stable mesoporous aluminosilicates (MSU-S) assembled from zeolite seeds as catalysts for biomass pyrolysis. Microporous and Mesoporous Materials, 99(1-2), 132–139.